Acta Cryst. (1995). A**51**, 295–300

The Inverse Fourier Problem in the Case of Poor Resolution in One Given Direction: the Maximum-Entropy Solution

BY R. J. PAPOULAR

Brookhaven National Laboratory, Upton, NY 11973, *USA, and CEN Saclay, Laboratoire commun CEA-CNRS,* 91191 *Gif-sur-Yvette CEDEX, France*

AND A. ZHELUDEV, E. RESSOUCHE AND J. SCHWEIZER

CEA, Département de la Recherche Fondamentale sur la Matière Condensée/SPSMS/MDN, 17 *rue des Martyrs,* 38054 *Grenoble CEDEX* 9, *France*

(*Received* 13 *June* 1994; *accepted* 19 *August* 1994)

Abstract

When density distributions in crystals are reconstructed from 3D diffraction data, a problem sometimes occurs when the spatial resolution in one given direction is very small compared to that in perpendicular directions. In this case, a 2D projected density is usually reconstructed. For this task, the conventional Fourier inversion method only makes use of those structure factors measured in the projection plane. All the other structure factors contribute zero to the reconstruction of a projected density. On the contrary, the maximum-entropy method uses all the 3D data, to yield 3D-enhanced 2D projected density maps. It is even possible to reconstruct a projection in the extreme case when not one structure factor in the plane of projection is known. In the case of poor resolution along one given direction, a Fourier inversion reconstruction gives very low quality 3D densities 'smeared' in the third dimension. The application of the maximum-entropy procedure reduces the smearing significantly and reasonably well resolved projections along most directions can now be obtained from the MaxEnt 3D density. To illustrate these two ideas, particular examples based on real polarized neutron diffraction data sets are presented.

Introduction

Diffraction techniques are widely used for the investigation of microscopic density distributions in crystals (charge, spin *etc.*). These methods essentially provide information about the Fourier components of the density to be determined. Consequently, the inverse Fourier (IF) reconstruction plays a key role in the data-treatment procedures (see, for instance, Buerger, 1960). For example, in a polarized neutron diffraction experiment, one measures the so-called flipping ratios R of Bragg reflections hkl from a single-crystal sample. From the $R(hkl)$'s, the Fourier components of the periodic spin (magnetization) density $S(\mathbf{r})$ in the crystal (the magnetic structure factors) $F_M(hkl)$ may be deduced. These are related to $S(\mathbf{r})$ by

$$F_M(hkl) = \int S(r) \exp[2\pi i(hx + ky + lz)] \mathrm{d}^3\mathbf{r}, \quad \mathbf{r} = (x, y, z). \tag{1}$$

Several different approaches to solving the IF problem exist. One of them consists in constructing a parametrized model of the density and refining the parameters to best fit the experimental diffraction data. For example, the spin density may be expanded into a multipolar series around the nuclei (Gillon & Schweizer 1989). The number of parameters in the model should be less (desirably much less) than the number of data. Devising such a model implies additional assumptions regarding what the reconstructed density should be like *via* the parameters required to describe it.

Direct model-independent methods, which are the concern of this paper, use no knowledge of what the spin density should look like and reconstruct the density distribution using no information but the experimental data. The most straightforward direct approach, Fourier synthesis (Fourier inversion), has been widely used for diffraction data treatment. One calculates the inverse Fourier sum including only those coefficients that have been measured:

$$S(\mathbf{r}) = (1/V) \sum_{h,k,l} F_M(hkl) \exp[-2\pi i(hx + ky + lz)]. \tag{2}$$

Implementations of direct methods may use many more variables than data, such as the values of the density in pixels of a grid in the direct space. For this reason and since the experimental data are never complete (only a part of the Fourier components may be experimentally measured), the solution to the IF problem is not unique:

(i) All the density distributions (maps) within some reasonable range of agreement with experiment (for example, which correspond to $\chi^2 \leq N_{\text{obs}}$, the number of observed structure factors) are acceptable.

ISSN 0108-7673

(ii) An acceptable map may correspond to any values of unmeasured Fourier components. Thus, a logical criterion is required to choose the 'best' map among all those consistent with experiment.

Fourier inversion selects one particular spatial density among all those consistent with the data in a rather arbitrary (not necessarily 'best') way:

(i) The Fourier density has exactly zero values for the unmeasured Fourier coefficients. This introduces into the reconstructed density spatial correlations for which there is no experimental evidence.

(ii) Those coefficients measured are taken by Fourier inversion exactly in the center of the experimental error bars, rejecting the important information contained in the latter. Indeed, the standard Fourier inversion procedure can be generalized to incorporate error bars (Papoular, 1992), but this improvement alone does not help much.

By contrast, the maximum-entropy (MaxEnt) method (Gull & Daniell, 1978; Skilling & Gull, 1985) was a significant advance in inverse problem solving. This approach is better justified from the point of view of information theory. It allows one to eliminate artifact features, use the information contained in the experimental error bars and reduce image smearing. Since the work of Collins (1982), MaxEnt has been widely used in crystallography to reconstruct densities (see, for instance, Sakata & Sato, 1990; Sakata, Mori Kumazawa & Takata, 1990; Sakata, Uno, Takata & Mori, 1992; Sakata, Uno, Takata & Howard, 1993; Papoular & Schweizer, 1991; Papoular, Prandl & Schliebel, 1992; Papoular & Gillon, 1990*b*; Papoular, 1992; Papoular, Roth, Heger, Haluska & Kuzmany, 1993; Papoular & Delapalme, 1994). It turned out to be very useful for spin-density reconstruction from polarized neutron diffraction data (Papoular & Gillon, 1990*a*; Papoular & Schweizer, 1991; Papoular & Delapalme, 1994).

Both Fourier inversion and maximum entropy are regularization procedures (Press, Teukolskey, Vetterling & Flannery, 1992). The superiority of MaxEnt comes from its nonlinear character and its ability to provide the least correlated density compatible with the data (Livesey & Skilling, 1985) as well as to take prior knowledge into account whenever available. In practice, one writes

$$\begin{aligned} \text{Entropy}[S(\mathbf{r})] &= -\int s(\mathbf{r}) \ln[s(\mathbf{r})] \mathrm{d}\mathbf{r} \\ s(\mathbf{r}) &= S(\mathbf{r}) / \int S(\mathbf{r}) \mathrm{d}\mathbf{r} \end{aligned} \tag{3}$$

and the historic MaxEnt algorithm (Gull & Skilling 1989) is utilized. One maximizes the functional (3) for a density distribution defined at points of a grid that splits the crystallographic unit cell into pixels. A conditional maximum, satisfying some criterion of consistency with the experimental data is the MaxEnt solution. In the 'historical' MaxEnt algorithm, this criterion is chosen simply as $\chi^2 \leq N_{\text{obs}}$, which, because (3) is a concave functional, is equivalent to a stricter constraint $\chi^2 = N_{\text{obs}}$. Not only is the MaxEnt choice more justified in the sense of information theory, but the quality of the density reconstructions is greatly increased.

Reconstruction of a projected spin density

In many cases, one can only reconstruct a crystallographic projection of the scattering density. This may be due to certain limitations in the experimental geometry. Such limitations are typical for polarized neutron diffraction experiments. In the latter, the periodic spin density is induced in a single-crystal sample by applying a strong magnetic field of a cryomagnet at sufficiently low temperature. Owing to the construction of the cryostat, the applied field is in the vertical (z) direction. The incident neutron beam is in the horizontal plane. The detector of the diffracted beam is basically in the horizontal plane as well. It may be lifted above the plane but only up to a certain angle. The limit is imposed by the construction of the cryocoil. As a result, only a 'thick layer' in reciprocal space is accessible for measurements. If the crystal is mounted in the cryostat with the c axis vertical, parallel to the applied field, typically only $hk0$, $hk1$ and $hk2$ flipping ratios may be measured. As a result, the spatial resolution along the c direction is very low. Nevertheless, a projection onto the ab crystallographic plane may be obtained. For this, the Fourier inversion formula may be applied:

$$\begin{aligned} S(x, y) &= \int S(\mathbf{r}) \mathrm{d}z \\ &= A^{-1} \sum_{h,k} F_M(hk0) \exp[-2\pi i (hx + ky)], \end{aligned} \tag{4}$$

where A is the projected surface of the unit cell. Note that only the in-plane $hk0$ Fourier components are included in this sum. The 2D reconstruction may be improved by using the MaxEnt procedure, but still only a part of the data collected is then being used.

We shall demonstrate that all the 3D data may and should be used for the reconstruction of 2D projections. For this, first, a complete 3D spin density in the crystal is reconstructed using MaxEnt. The obtained density is then projected along the c axis. Owing to the non-linear

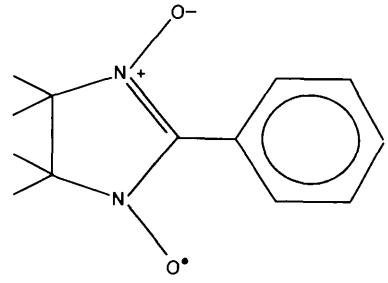

Fig. 1. Structural formula of PNN, the phenyl-substituted α-nitroso-nitroxide free radical.

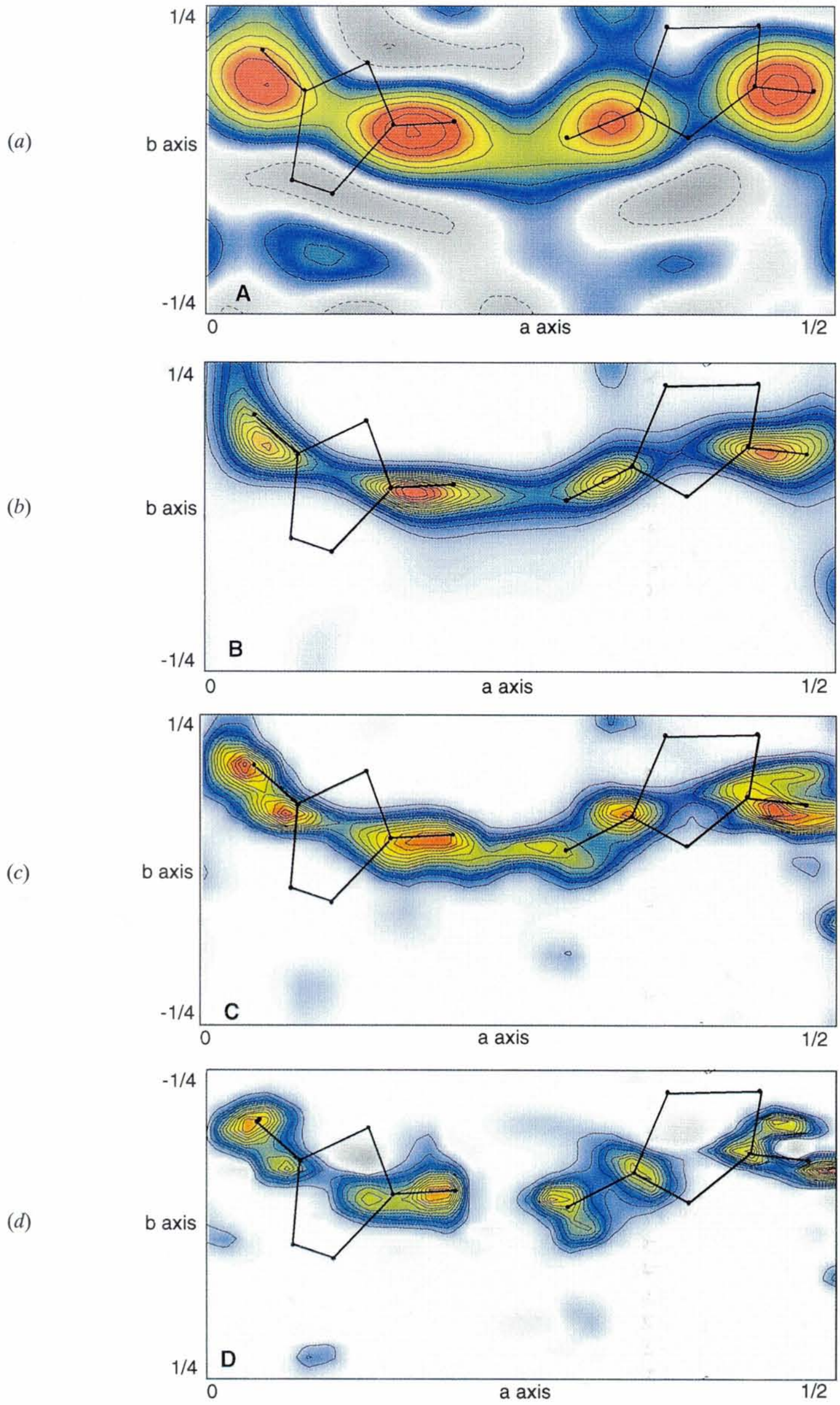

Fig. 2. Spin density in the PNN crystal in projection onto the *ab* crystallographic plane. (*a*) 0.0125$\mu\beta$ Å2 and (*b*)–(*d*) 0.025 $\mu\beta$ Å2 contours, negative contours dashed. False color (positive densities) and grayscale (negative). (*a*) Direct inversion from 42 *hk0* Fourier data. (*b*) 2D MaxEnt from 42 *hk0* data. (*c*) 3D MaxEnt using 187 *hkl* data. (*d*) 3D MaxEnt using 145 *hkl*, l≠0 data.

dependence of the 3D MaxEnt density on the structure factors, the contribution of the *hk*1, *hk*2 *etc.* reflections do not cancel out any longer on projection and do contribute to the reconstruction of the projected density.

A worked-out example

To illustrate the efficiency of the new technique, we shall demonstrate its application to the reconstruction of the spin density in an organic free-radical crystal, the phenyl-substituted α-nitrosonitroxide PNN (Fig. 1). This compound is paramagnetic owing to an unpaired electron residing in the π^* molecular orbital, which has strong contributions from the atomic p orbitals of the NO-group atoms. Thus, in the crudest molecular-orbital model, the spin density is expected to be localized on these atomic sites. To find out how exactly the spin density is distributed within the molecule, we performed a single-crystal polarized neutron diffraction experiment (Ressouche *et al.*, 1993; Zheludev *et al.*, 1994). PNN crystallizes in the monoclinic space group $P2_1/c$ ($a = 20.871$, $b = 10.150$, $c = 12.130$ Å and $\beta = 107.15°$). The asymmetric unit cell contains two crystallographically independent PNN molecules. A periodic magnetization was induced in a single-crystal sample by means of a $H = 8$ T external field at $T = 5$ K. The crystal was mounted with the c axis vertical, parallel to the field. 187 flipping ratios (all in the reciprocal-space planes $0 \leq l \leq 3$), of which 42 were of the type (*hk*0), that is in the horizontal plane, were collected.

Fig. 2(*a*) shows the spin density in projection onto the *ab* crystallographic plane reconstructed by Fourier inversion (4). The main features (a strong contribution from the NO groups) are visible, but the quality of the reconstruction is unsatisfactory because: (i) a significant density is located at some points rather far from the nuclei. This is unphysical and obviously is an artifact; (ii) the image is smeared out, since in the diffraction experiment the measurements have been performed only up to a certain value of $\sin\theta/\lambda_{max} = 0.42$ Å^{-1} and only the low-**k** components have been included in (4).

A 2D historic MaxEnt 32×32 grid was used to reconstruct the same density from the 42 (*hk*0) structure factors. The result is shown in Fig. 2(*b*). The improvement is obvious, the artifacts have disappeared and the image is less smeared.

Then all the 187 *hkl* structure factors were used to reconstruct a 3D density using historic MaxEnt on a $32 \times 32 \times 32$ array of pixels. This density was then

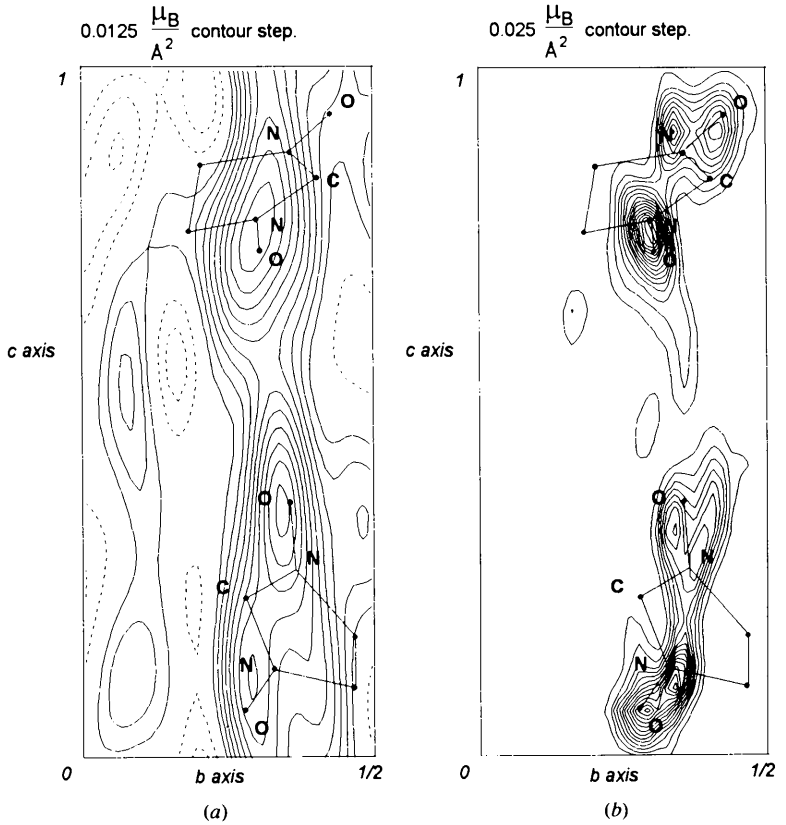

Fig. 3. Spin density in PNN crystal in projection onto the *bc* crystallographic plane. (*a*) $0.0125\,\mu_B$ Å^{-2} and (*b*) $0.025\,\mu_B$ Å^{-2} contours, negative contours dashed. (*a*) Direct Fourier inversion. (*b*) 3D MaxEnt. 187 *hkl*, $0 \leq l \leq 3$.

projected onto the *ab* crystallographic plane using (4). The quality of the reconstruction (Fig. 2*c*) is much higher. The individual atoms within the NO groups are now discernible.

It is important to emphasize that the same procedure, reconstructing a 3D density and projecting it in 2D, would not work with Fourier inversion. In fact, it would yield exactly the same map as presented in Fig. 2(*a*) since all the contributions of Fourier components other than *hk*0 would be integrated out on projection.

In principle, the grid resolution should be chosen in such a way that the size of each pixel be small compared to the experimental resolution, as well as to the size of possible features of physical/chemical interest. An extra justification for using small-sized pixels is to lessen rounding errors when other projections than the one along the *c* axis are sought. In the reconstruction described above, the pixel dimensions are $0.33 \times 0.16 \times 0.38\,\text{Å}^3$, which should be compared to $\lambda_{max}/\sin\theta = 2.4\,\text{Å}$.

The power of the new method is best demonstrated by the following striking example. We have artifically removed all the *hk*0 structure factors from the data set. In this case, Fourier inversion yields a flat featureless projected density $[S(x, y) = 0]$. Since no 2D data are given, this is also the case with 2D MaxEnt, which selects the most probable answer in the absence of data – again a flat density. These methods are incapable of using the 3D data available. On the contrary, '3D MaxEnt+ projection' reconstructs the main features of the projected density using the 145 out-of-plane data as shown in Fig. 2(*d*). The map speaks for itself: 3D MaxEnt is a far better way to extract all the information contained in the data.

Reconstruction of 3D densities

In the case when only a 'thick layer' in reciprocal space is accessible for measurements, the resolution along the *z* axis is very low and 3D densities obtained by Fourier inversion are extremely smeared in that direction. In this case, the Fourier inversion method is inadequate for 3D reconstructions. This is illustrated in Fig. 3(*a*), which shows a projection of a 3D Fourier inversion map obtained for PNN onto the *bc* crystallographic plane. The quality of the reconstruction is much lower since the resolution along **c** is very limited, $0 \le l \le 3$. Even individual NO groups are indiscernible.

Applying the MaxEnt procedure reduces the smearing, since no long-range spatial correlations are now imposed by forcing all the $l > 3$ Fourier components to be equal to zero. The 3D MaxEnt map in projection onto the *bc* plane is shown in Fig. 3(*b*). Reducing smearing is just the desired effect for spin (or charge) densities, which are expected to be localized around the nuclei. The effective resolution in the third dimension is thus increased.

Non-crystallographic projections

Since MaxEnt offers a much enhanced resolution in three dimensions, any desired projection or section (not necessarily crystallographic) may be sought. This is illustrated by the following example.

To obtain a better view of the spin distribution in PNN, a parallelepipedal 'box' of dimensions $4.5 \times 7.0 \times 4.0\,\text{Å}$ containing one of the two molecules was defined. Fig. 4 shows the 3D MaxEnt spin density confined in this box in projection onto one of the rectangular box faces (the *XY* plane, which is chosen parallel to the molecular O—N—C—N—O plane of the radical; the direction of orthogonal projection is the *Z* axis). To obtain this projection, a trivial extrapolation of the MaxEnt density (defined in a discrete set of cells of a $32 \times 32 \times 32$ crystallographic 3D grid) to other points of space was performed. The value corresponding to each cell of the grid was simply assigned to all the points of space contained within that cell. The projection was then calculated as an integral along *Z* of the thus-defined function of space. The integration procedure used a 50×50 2D grid in the *XY* plane and 100 integration points along *Z*.

Concluding remarks

MaxEnt can and should be used for the reconstruction of scattering densities from diffraction data. It allows one to select the most probable answer for a given data set and a given prior knowledge of the sought density (chosen to be uniform in this paper). It is a model-independent method, which does not impose any rigid constraints on the density to be reconstructed.

The new 3D MaxEnt is a new step in polarized neutron diffraction data treatment: (i) it allows one to use all the 3D data available to reconstruct 2D crystallographic projections; (ii) a projection may be recon-

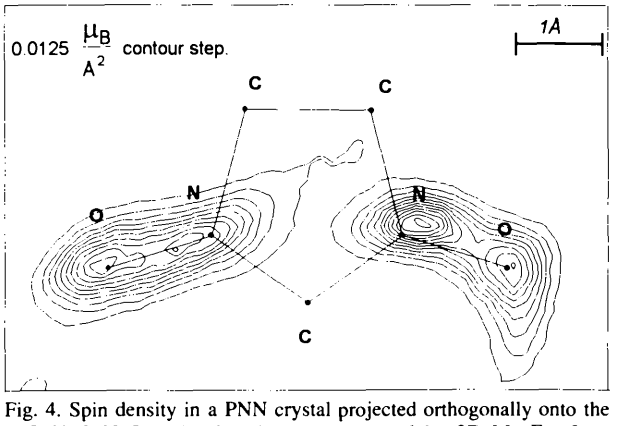

Fig. 4. Spin density in a PNN crystal projected orthogonally onto the O–N–C–N–O molecular plane reconstructed by 3D MaxEnt from 187 *hkl* Fourier components. $0.0125\,\mu_B\,\text{Å}^{-2}$ contours, negative contours dashed.

structed even if not one structure factor in the projection plane can be measured; (iii) it increases significantly the effective resolution in the third dimension, making considerably enhanced 3D reconstructions and non-crystallographic projections possible.

References

BUERGER, M. J. (1960). *Crystal Structure Analysis*, ch. 14, pp. 380–384. New York: John Wiley.

COLLINS, D. M. (1982). *Nature (London)*, **29B**, 49–51.

GILLON, B. & SCHWEIZER, J. (1989). *Study of Chemical Bonding in Molecules: the Interest of Polarized Neutron Diffraction*, edited by J. MARUANI. *Molecules in Physics, Chemistry and Biology*, Vol. II, pp. 111–147. Dordrecht: Kluwer Academic Publishers.

GULL, S. F. & DANIELL, G. J. (1978). *Nature (London)*, **272**, 686–690.

GULL, S. F. & SKILLING, J. (1989). *MEMSYS Users' Manual*. Maximum Entropy Data Consultants Ltd, 33 North End, Meldreth, Royston SG8 6NR, England.

LIVESEY, A. K. & SKILLING, J. (1985). *Acta Cryst.* A**41**, 113–122.

PAPOULAR, R. J. (1992). *Acta Cryst.* A**48**, 244–246.

PAPOULAR, R. J. & DELAPALME, A. (1994). *Phys. Rev. Lett.* **72**, 1486–1489.

PAPOULAR, R. J. & GILLON, B. (1990*a*). *Neutron Scattering Data Analysis* 1990, edited by M. W. JOHNSON. *Inst. Phys. Conf. Ser.* No. 107, pp. 101–116.

PAPOULAR, R. J. & GILLON, B. (1990*b*). *Europhys. Lett.* **13**, 429–434.

PAPOULAR, R. J., PRANDL, W. & SCHIEBEL, P. (1992). *Maximum Entropy and Bayesian Methods*, edited by G. ERICKSON, C. RAY-SMITH & P. NEUDORFER, pp. 359–376. Dordrecht: Kluwer Academic Publishers.

PAPOULAR, R. J., ROTH, G., HEGER, G., HALUSKA, M. & KUZMANY, H. (1993). *Proceedings IWEP NM*93, edited by H. KUZMANY. *Springer Series in Solid State Sciences*, No. 117, pp. 189–194.

PAPOULAR, R. J. & SCHWEIZER, J. (1991). Proceedings of the 6th International Neutron School on Neutron Physics, Alushta, Russia, 8–18 October 1991, pp. 170–189.

PRESS, W. H., TEUKOLSKY, S. A., VETTERLING, W. T. & FLANNERY, B. P. (1992). *Numerical Recipes: the Art of Scientific Computing*, 2nd ed., pp. 795–817. Cambridge Univ. Press.

RESSOUCHE, E., ZHELUDEV, A., BOUCHERLE, J. X., GILLON, B., REY, P. & SCHWEIZER, J. (1993). *Mol. Cryst. Liq. Cryst.* **232**, 13–25.

SAKATA, M., MORI, R., KUMAZAWA, S. & TAKATA, M. (1990). *J. Appl. Cryst.* **23**, 526–534.

SAKATA, M. & SATO, M. (1990). *Acta Cryst* A**46**, 263–270.

SAKATA, M., UNO, T., TAKATA, M. & HOWARD, C. (1993). *J. Appl. Cryst.* **26**, 159–165.

SAKATA, M., UNO, T., TAKATA, M. & MORI, R. (1992). *Acta Cryst.* B**48**, 591–598.

SKILLING, J. & GULL, S. F. *Maximum Entropy and Bayesian Methods in Inverse Problems*, edited by C. RAY SMITH & W. T. GRANDY JR, pp. 83–132. Dordrecht: Reidel.

ZHELUDEV, A., BARONE, V., BONNET, M., DELLEY, B., GRAND, A., RESSOUCHE, E., REY, P., SUBRA, R. & SCHWEIZER, J. (1994). *J. Am. Chem. Soc.* **116**, 2019–2027.

Acta Cryst. (1995). A**51**, 300–304

Über isomorphe Untergruppen von Raumgruppen der Kristallklassen 4, $\bar{4}$, $4/m$, 3, $\bar{3}$, 6, $\bar{6}$ und $6/m$

VON ULRICH MÜLLER

Fachbereich Biologie/Chemie, Universität-GH, D-34109 Kassel, Deutschland

UND ACHIM BRELLE

Fachbereich Mathematik/Informatik, Universität-GH, D-34109 Kassel, Deutschland

(*Eingegangen am* 18. *August* 1994, *angenommen am* 3. *November* 1994)

Abstract

Number theory is used to derive which indices of symmetry reduction can occur for maximal isomorphic subgroups of space groups belonging to the crystal classes mentioned in the title and having unit cells with enlarged base vectors **a** and **b**. In the case of the crystal classes 4, $\bar{4}$ and $4/m$, the possible index values are $i = p^2$ with $p \equiv 3 \pmod 4$, $i = 2$ and $i = p \equiv 1 \pmod 4$ (p = prime number). In the crystal classes 3, $\bar{3}$, 6, $\bar{6}$ and $6/m$, $i = p^2$ with $p \equiv 2 \pmod 3$, $i = 3$ and $i = p \equiv 1 \pmod 3$ are possible. The number of isomorphic subgroups of index i (maximal and non-maximal) can be calculated with the formula $R(i) = \sum \chi_D(m)$, where m runs through all divisors of i and $\chi_D(m)$ is the Dirichlet character mod $|D|$; $D = -4$ for the tetragonal and $D = -3$ for the trigonal and hexagonal space groups. $\chi_{-4}(m)$ is equal to 0 for $m \equiv 0 \pmod 2$, 1 for $m = p \equiv 1 \pmod 4$, -1 for $m = p \equiv 3 \pmod 4$, and the corresponding product for nonprime values of m. $\chi_{-3}(m)$ is equal to 0 for $m \equiv 0 \pmod 3$, 1 for $m = p \equiv 1 \pmod 3$, -1 for $m = p \equiv 2 \pmod 3$, and their corresponding product for nonprime m. $R(i)$ is the number of conjugacy classes, each of which comprises i conjugate subgroups (for $i > 2$).

Einleitung

Das auf Hermann (1960) zurückgehende und von Bärnighausen (1980) entwickelte Konzept zum Aufzei-